Supplement of Atmos. Chem. Phys., 17, 327–342, 2017
http://www.atmos-chem-phys.net/17/327/2017/
doi:10.5194/acp-17-327-2017-supplement

Atmospheric Chemistry and Physics
Open Access
EGU

Supplement of

Dynamic subgrid heterogeneity of convective cloud in a global model: description and evaluation of the Convective Cloud Field Model (CCFM) in ECHAM6–HAM2

Zak Kipling et al.

Correspondence to: Zak Kipling (zak.kipling@physics.ox.ac.uk)

1 CCFM in standard ECHAM (without HAM)

The simulations using standard ECHAM were at T63L47 (same tropospheric vertical resolution as ECHAM–HAM but extended to 0.01 hPa, with a 2×10-minute leapfrog timestep), as described in Stevens et al. (2013). The reason for this is that the supported resolutions for ECHAM and ECHAM–HAMMOZ differ, and using a supported choice for each ensures that both control simulations are comparable with those carried out elsewhere. In these simulations, aerosols are taken from the MAC climatology (Kinne et al., 2013).

References

Kinne, S., O'Donnel, D., Stier, P., Kloster, S., Zhang, K., Schmidt, H., Rast, S., Giorgetta, M., Eck, T. F., and Stevens, B.: MAC-v1: A new global aerosol climatology for climate studies, Journal of Advances in Modeling Earth Systems, 5, 704–740, doi:10.1002/jame.20035, 2013.

Stevens, B., Giorgetta, M., Esch, M., Mauritsen, T., Crueger, T., Rast, S., Salzmann, M., Schmidt, H., Bader, J., Block, K., Brokopf, R., Fast, I., Kinne, S., Kornblueh, L., Lohmann, U., Pincus, R., Reichler, T., and Roeckner, E.: Atmospheric component of the MPI-M Earth System Model: ECHAM6, Journal of Advances in Modeling Earth Systems, 5, 146–172, doi:10.1002/jame.20015, 2013.

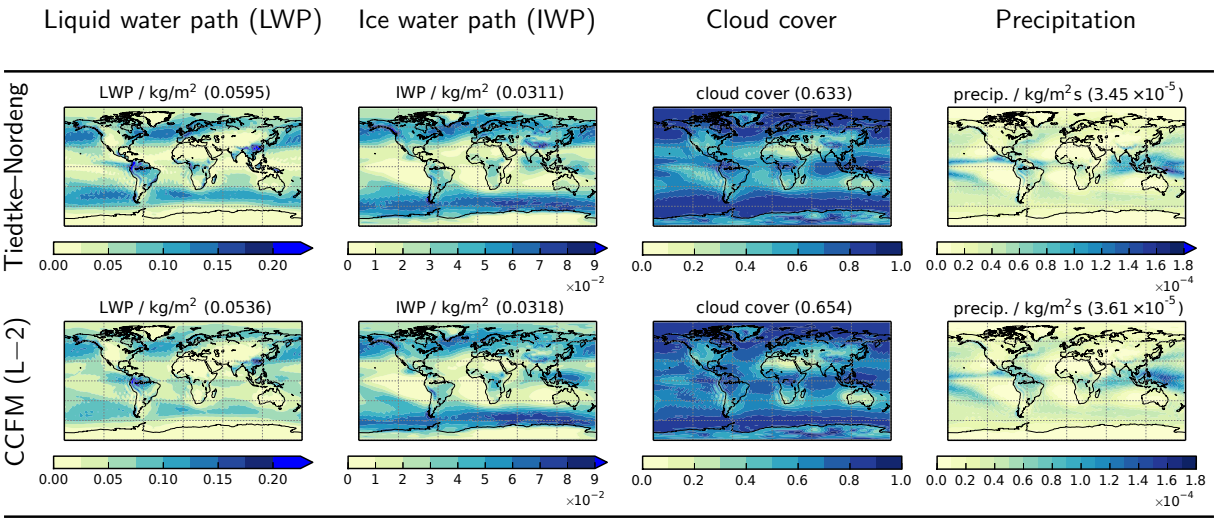

Figure S1: Annual mean (from left to right) liquid water path (LWP), ice water path (IWP), cloud cover and surface precipitation from 30-year AMIP-type simulations using ECHAM (without HAM) with Tiedtke–Nordeng and CCFM (L−2) convection. Note that the LWP and IWP scales are different from those in Figure 2 in the main article for ECHAM–HAM due to the quite different magnitudes. (The numbers in parentheses show the annual global mean of each quantity.)

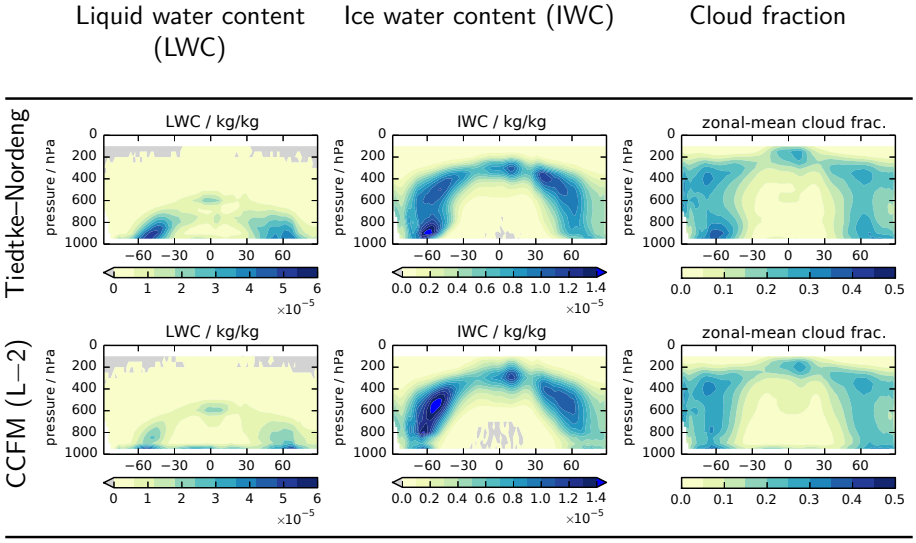

Figure S2: Annual and zonal mean (from left to right) liquid water content (LWC), ice water content (IWC) and cloud fraction from 30-year AMIP-type simulations using ECHAM (without HAM) with Tiedtke–Nordeng and CCFM (L−2) convection. Note that the LWC and IWC scales are different from those in Figure 3 in the main article for ECHAM–HAM due to their quite different magnitudes.

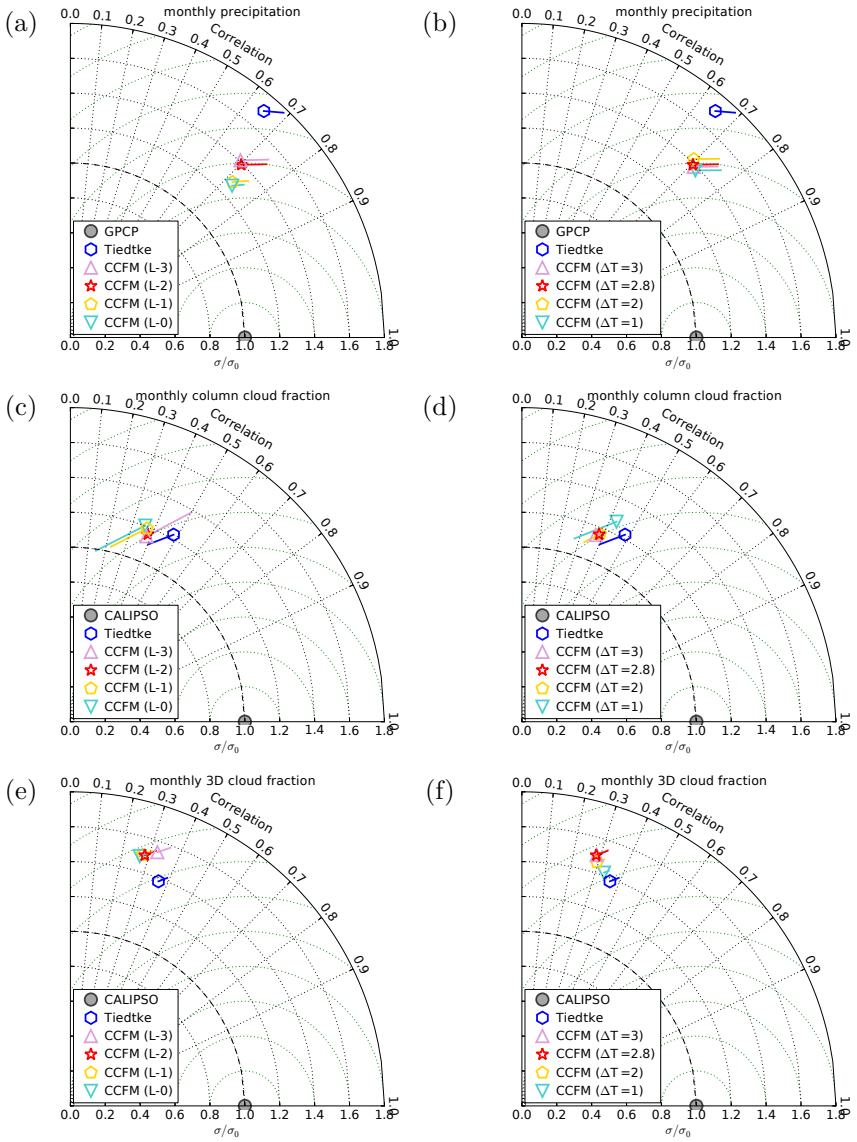

Figure S3: Taylor diagrams comparing (a,d) monthly mean precipitation, (b,e) COSP-simulated column cloud fraction, and (c,f) COSP-simulated 3D cloud fraction between one-year simulations using ECHAM–HAM with Tiedtke–Nordeng convection and with CCFM in each configuration, and the Global Precipitation Climatology Project (GPCP) and CALIPSO–GOCCP respectively. The left column (a–c) shows the use of different initiation levels in the CCFM sub-cloud model (all with a temperature perturbation of 2.8 K; the right column (d–f) shows the use of different temperature perturbations (all in L−2 configuration). The line segments extending from each point indicate the normalised mean bias as suggested in Taylor (2001).

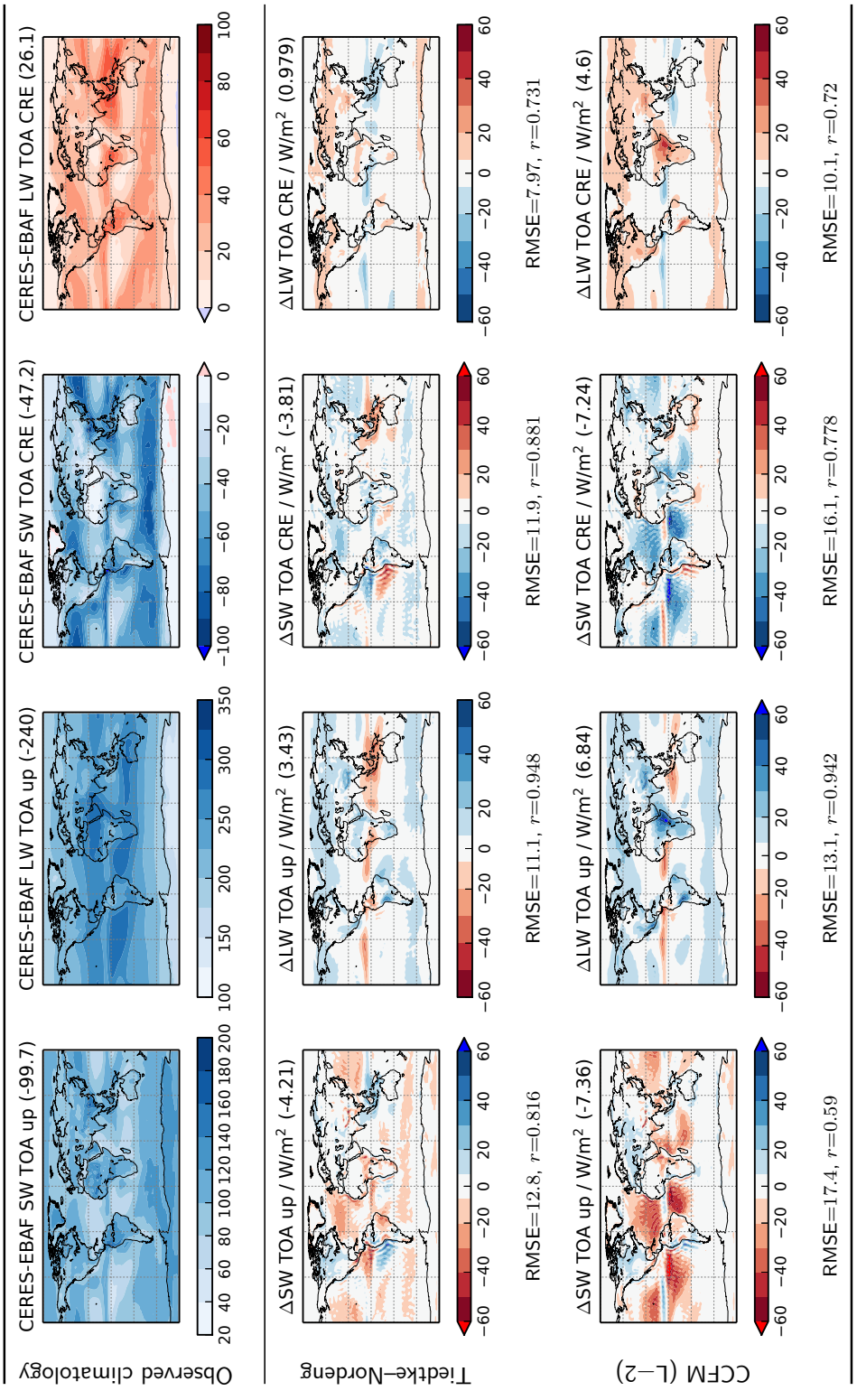

Figure S4: Difference in short- and long-wave upwelling radiative fluxes and cloud radiative effects at the top of the atmosphere between 30-year AMIP-type simulations using ECHAM–HAM with Tiedtke–Nordeng and CCFM (L−2) convection, and a CERES–EBAF climatology.

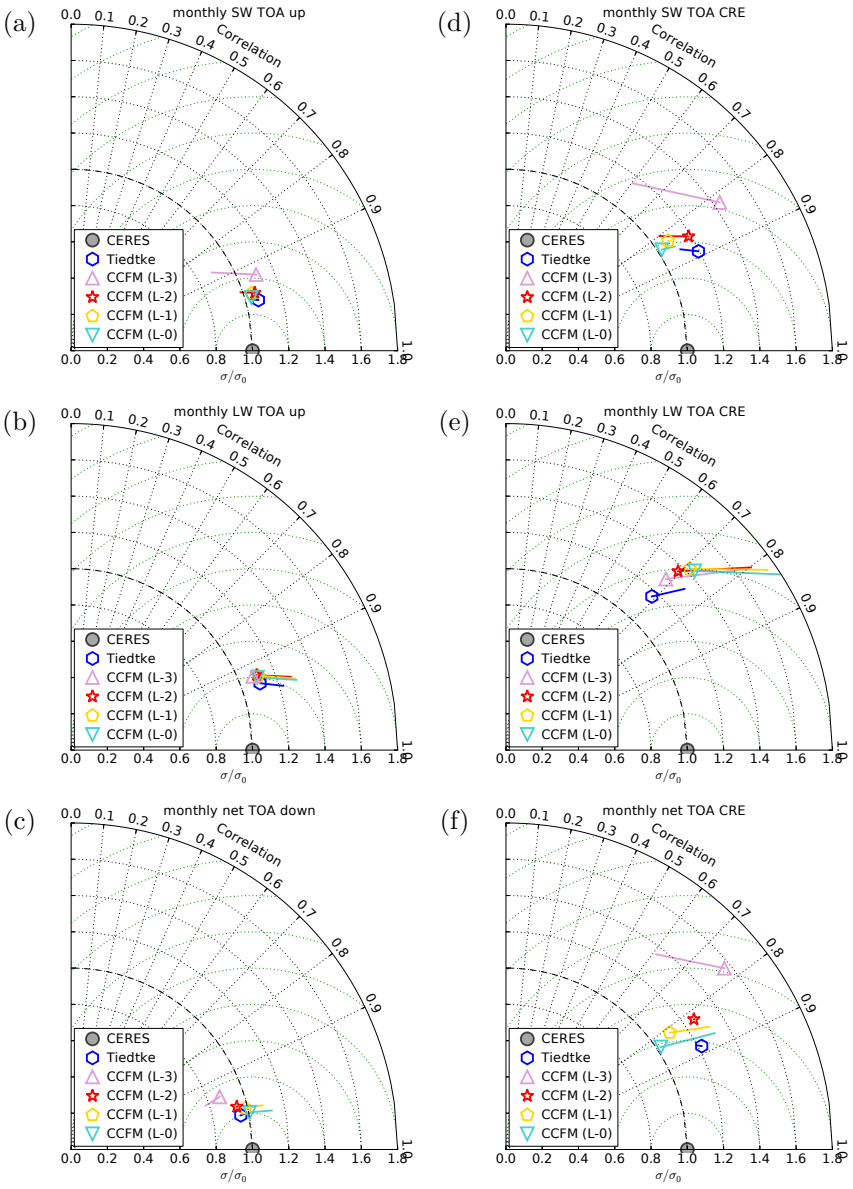

Figure S5: Taylor diagrams comparing monthly mean short-wave (a), long-wave (b) and net (c) radiative fluxes (left) and corresponding cloud radiative effects (right, d–f) at the top of the atmosphere between one-year simulations using ECHAM–HAM with Tiedtke–Nordeng convection and with CCFM in each configuration, and a CERES–EBAF climatology. The line segments extending from each point indicate the normalised mean bias as suggested in Taylor (2001).

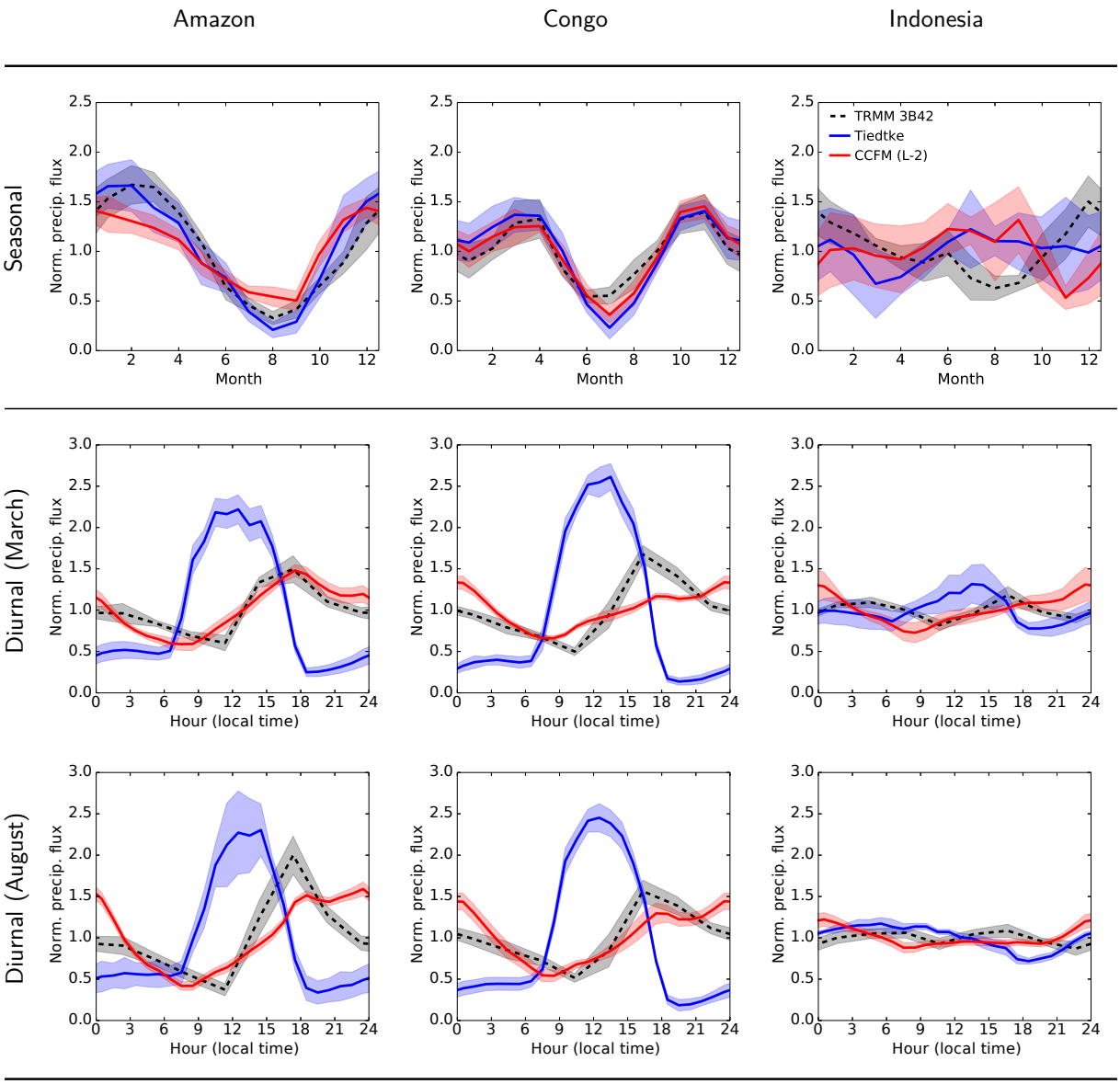

Figure S6: Normalised seasonal (top) and diurnal (below) cycles of precipitation in the Amazon (left), Congo (centre) and Indonesia (right) regions from a ten-year overlap between the TRMM 3B42 product and AMIP-type simulations using ECHAM (without HAM) with Tiedtke–Nordeng and CCFM (L−2) convection. The shaded regions indicate the interannual standard deviation of each data set. The dotted lines show the cycles from one-year simulations using alternative CCFM configurations. The diurnal cycles are in the local time of each region, and are shown for March and August; the full set of months is shown in Figures S10–12.

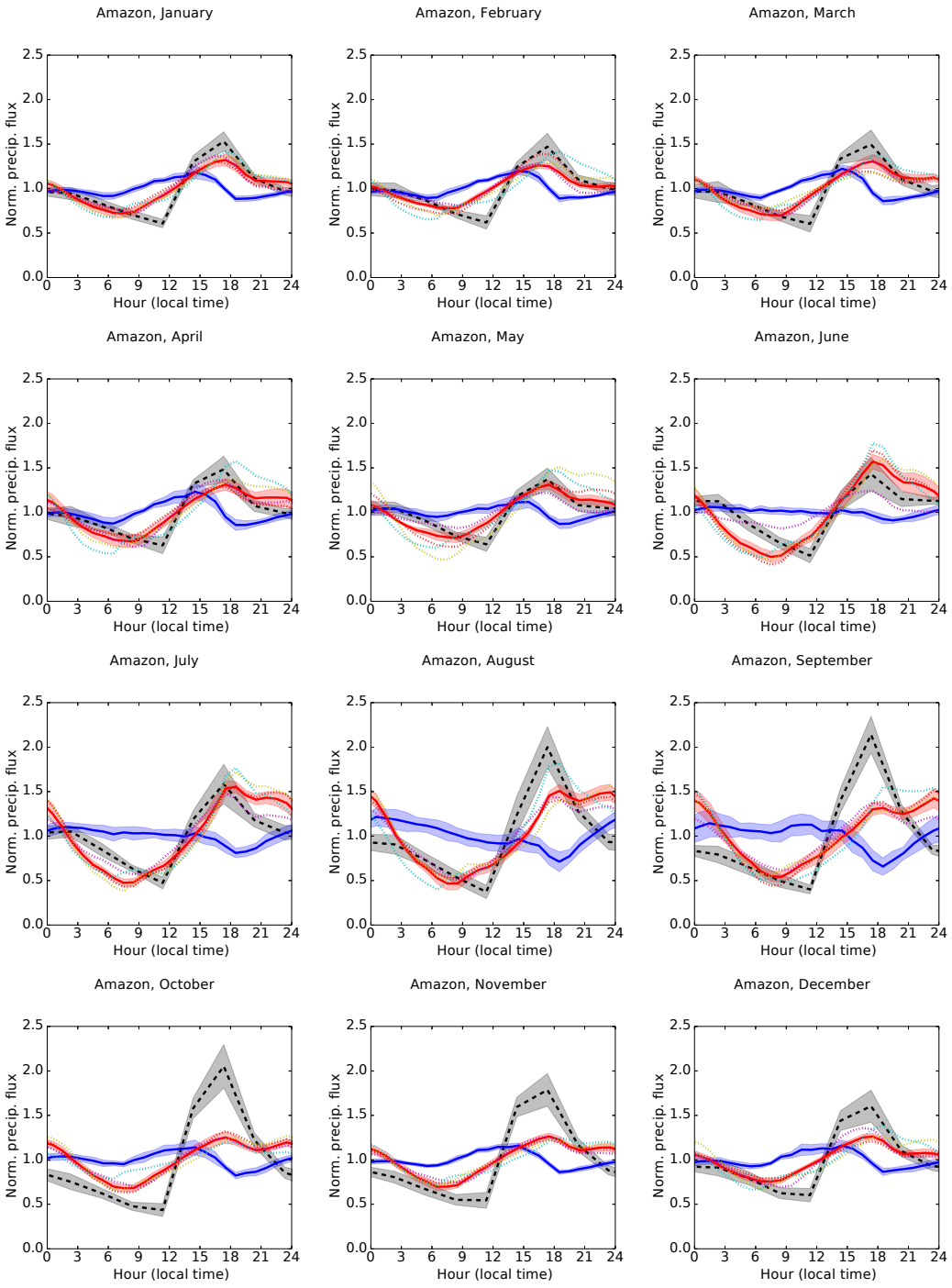

Figure S7: Normalised diurnal cycles of precipitation in the Amazon region from a ten-year overlap between the TRMM 3B42 product and AMIP-type simulations using ECHAM–HAM with Tiedtke–Nordeng and CCFM (L−2) convection. The shaded regions indicate the inter-annual standard deviation of each data set. The dotted lines show the cycles from one-year simulations using alternative CCFM configurations. The diurnal cycles are in the local time of each region. Line colours and styles as per Figure 9 in the main article.

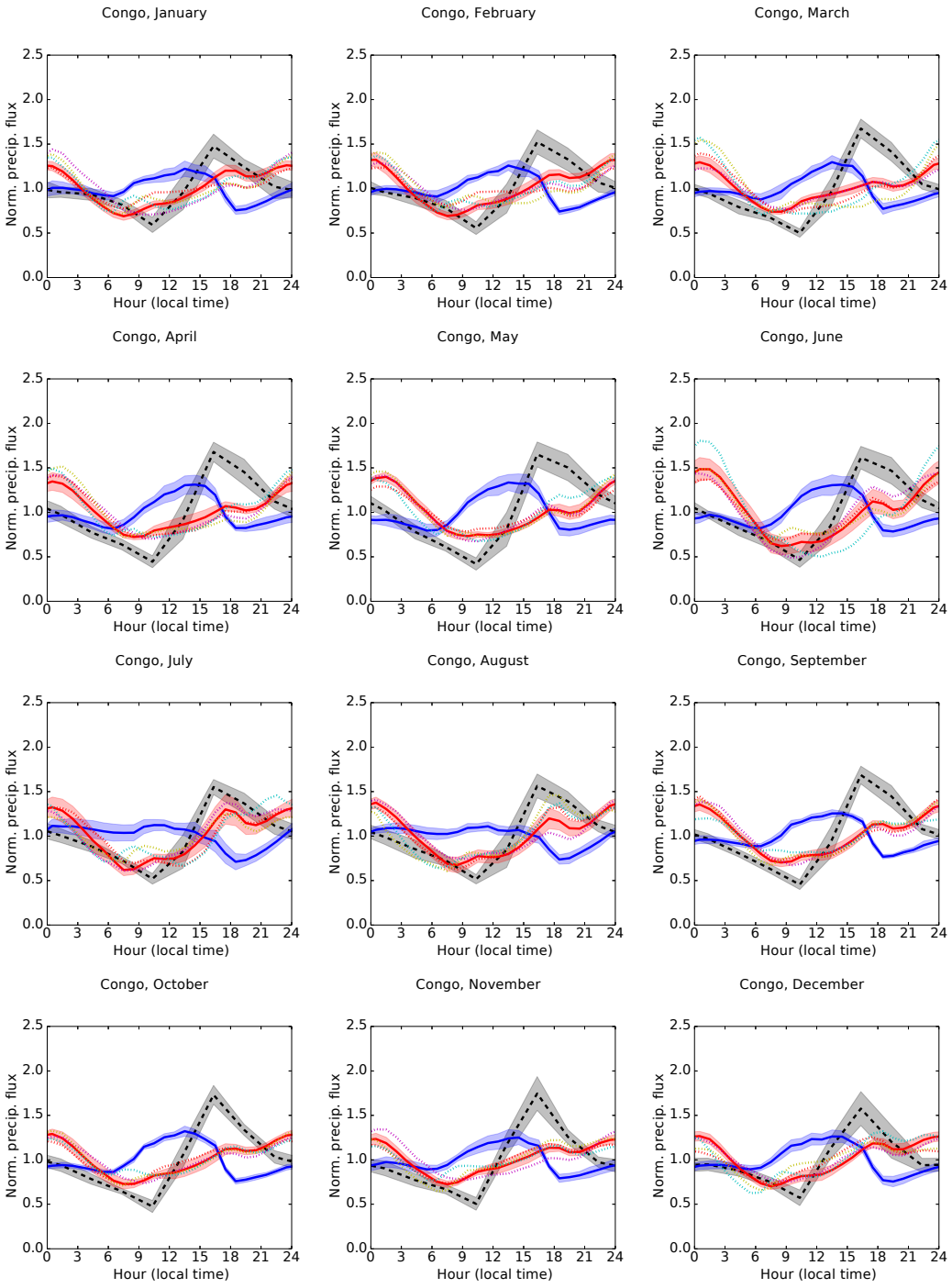

Figure S8: Normalised diurnal cycles of precipitation in the Congo region from a ten-year overlap between the TRMM 3B42 product and AMIP-type simulations using ECHAM–HAM with Tiedtke–Nordeng and CCFM (L−2) convection. The shaded regions indicate the interannual standard deviation of each data set. The dotted lines show the cycles from one-year simulations using alternative CCFM configurations. The diurnal cycles are in the local time of each region. Line colours and styles as per Figure 9 in the main article.

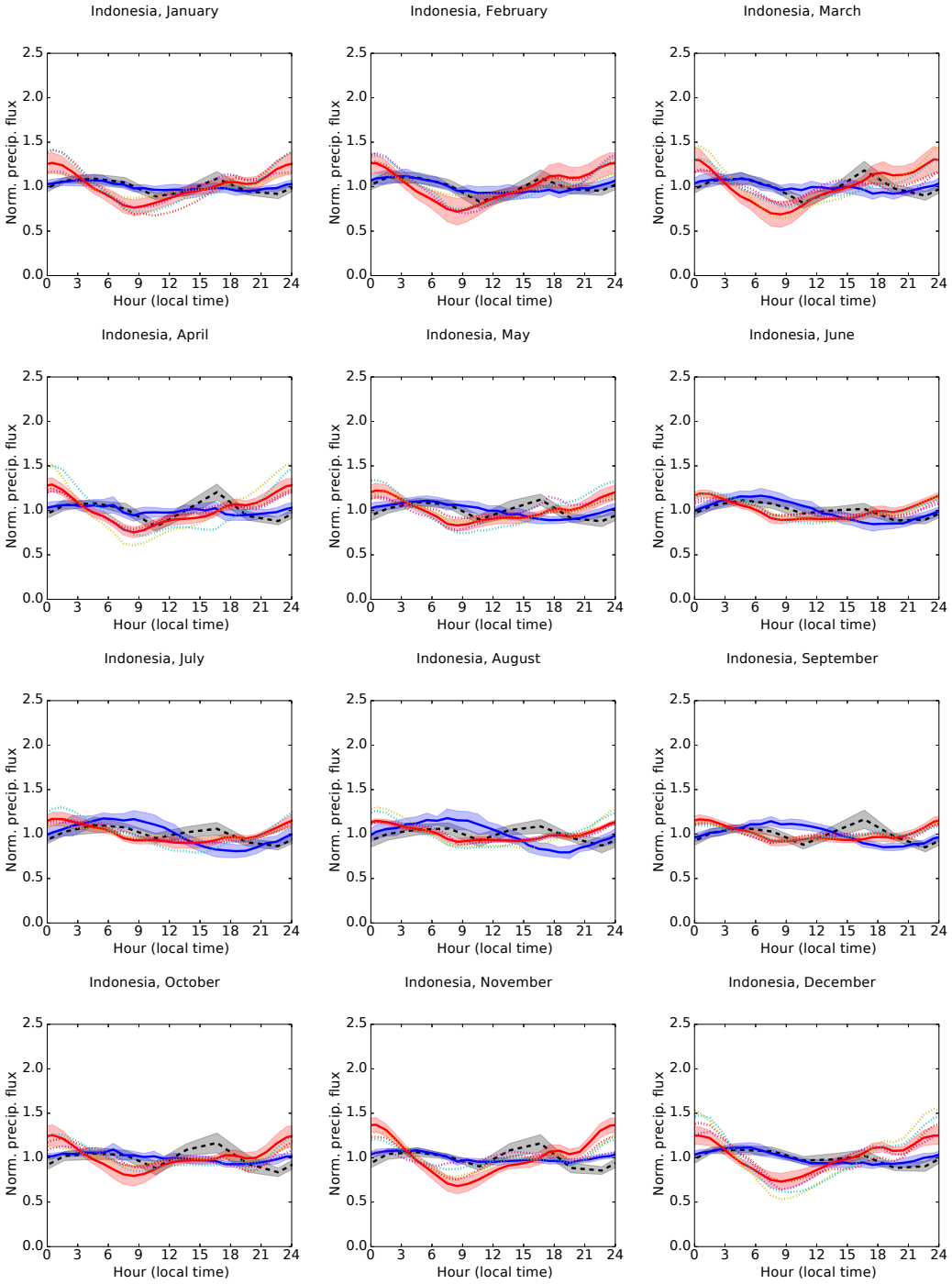

Figure S9: Normalised diurnal cycles of precipitation in the Indonesia region from a ten-year overlap between the TRMM 3B42 product and AMIP-type simulations using ECHAM–HAM with Tiedtke–Nordeng and CCFM (L−2) convection. The shaded regions indicate the inter-annual standard deviation of each data set. The dotted lines show the cycles from one-year simulations using alternative CCFM configurations. The diurnal cycles are in the local time of each region. Line colours and styles as per Figure 9 in the main article.

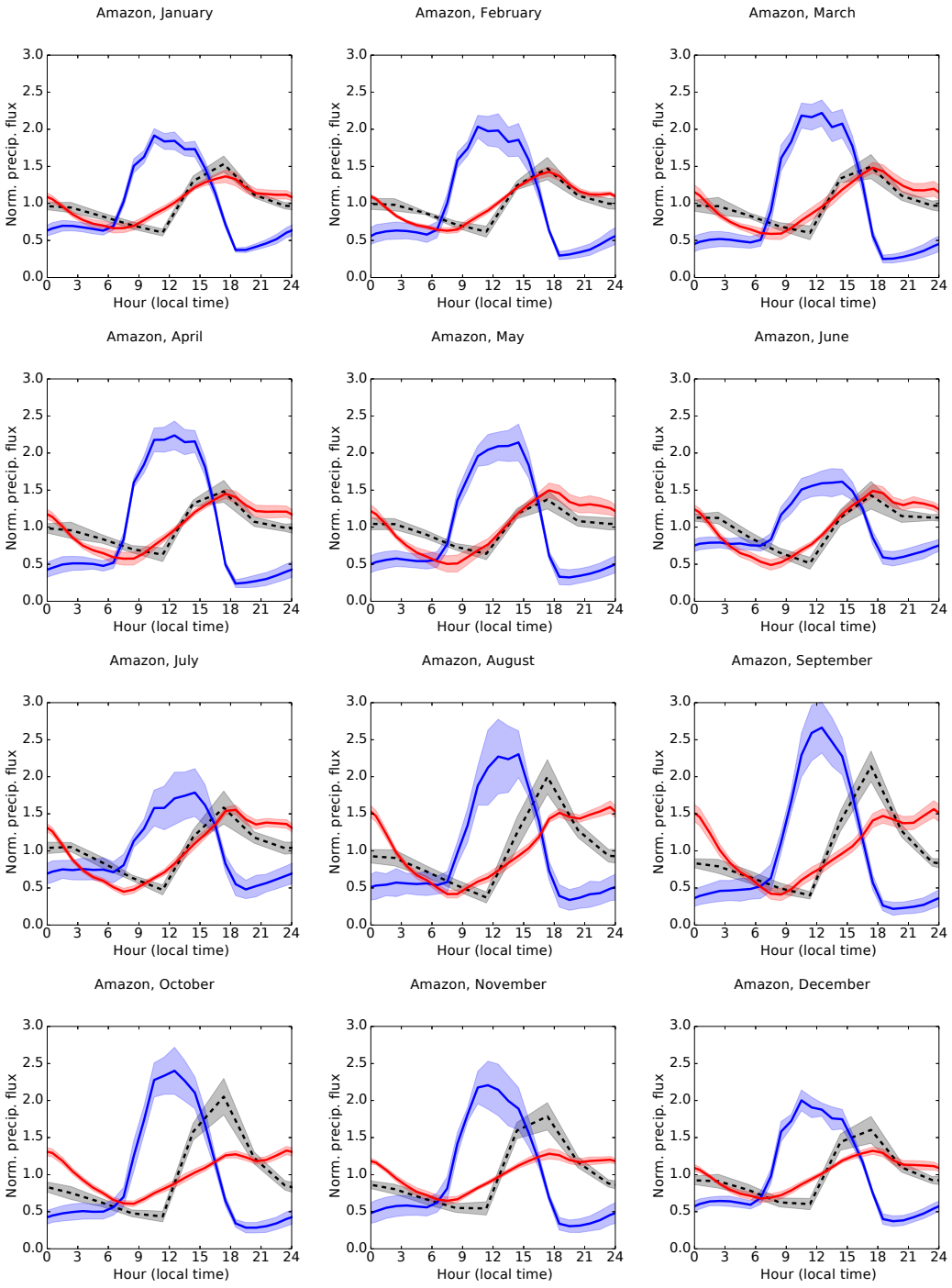

Figure S10: Normalised diurnal cycles of precipitation in the Amazon region from a ten-year overlap between the TRMM 3B42 product and AMIP-type simulations using ECHAM (without HAM) with Tiedtke–Nordeng and CCFM (L−2) convection. The shaded regions indicate the interannual standard deviation of each data set. The dotted lines show the cycles from one-year simulations using alternative CCFM configurations. The diurnal cycles are in the local time of each region. Line colours and styles as per Figure S6.

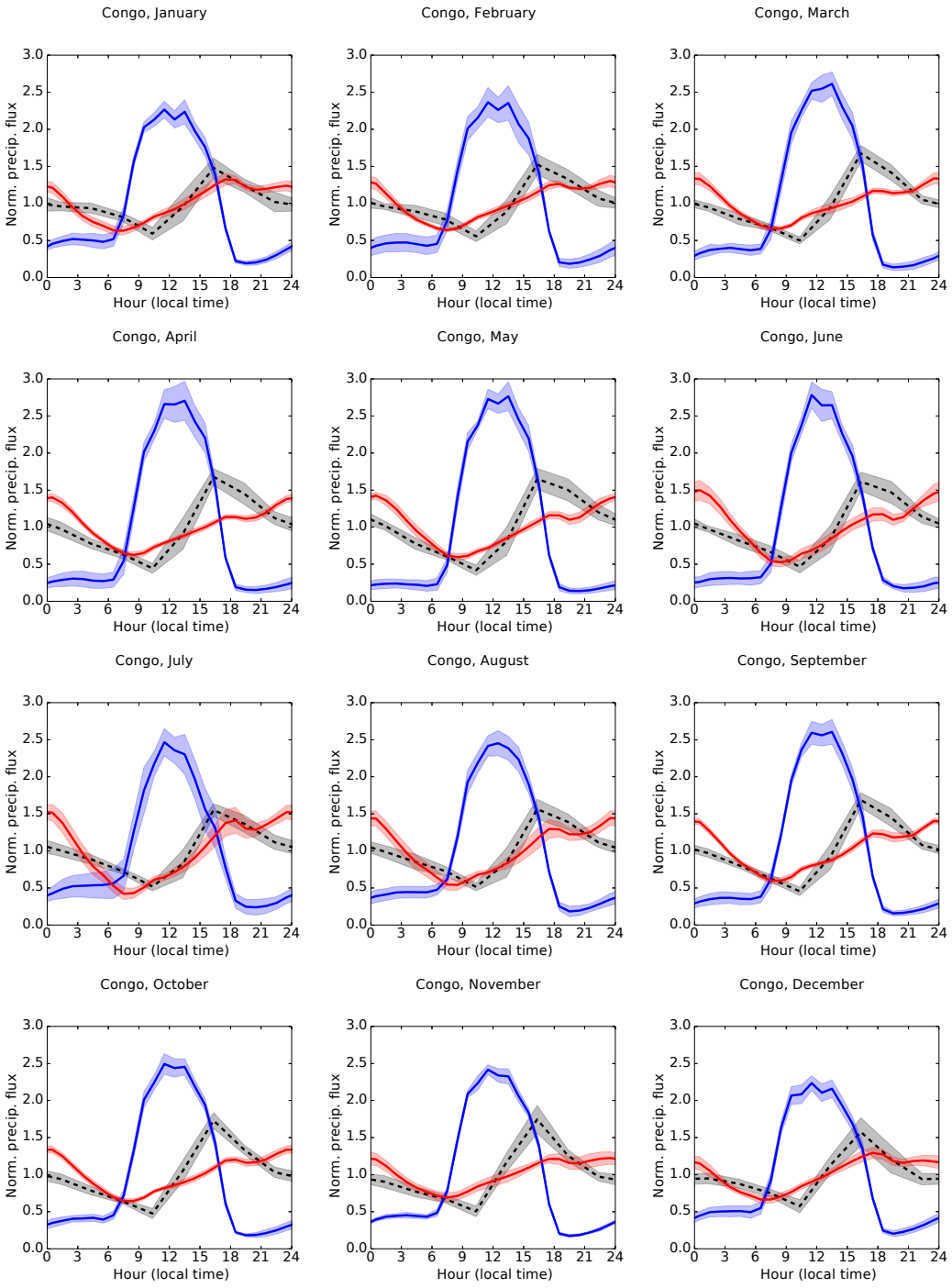

Figure S11: Normalised diurnal cycles of precipitation in the Congo region from a ten-year overlap between the TRMM 3B42 product and AMIP-type simulations using ECHAM (without HAM) with Tiedtke–Nordeng and CCFM (L−2) convection. The shaded regions indicate the interannual standard deviation of each data set. The dotted lines show the cycles from one-year simulations using alternative CCFM configurations. The diurnal cycles are in the local time of each region. Line colours and styles as per Figure S6.

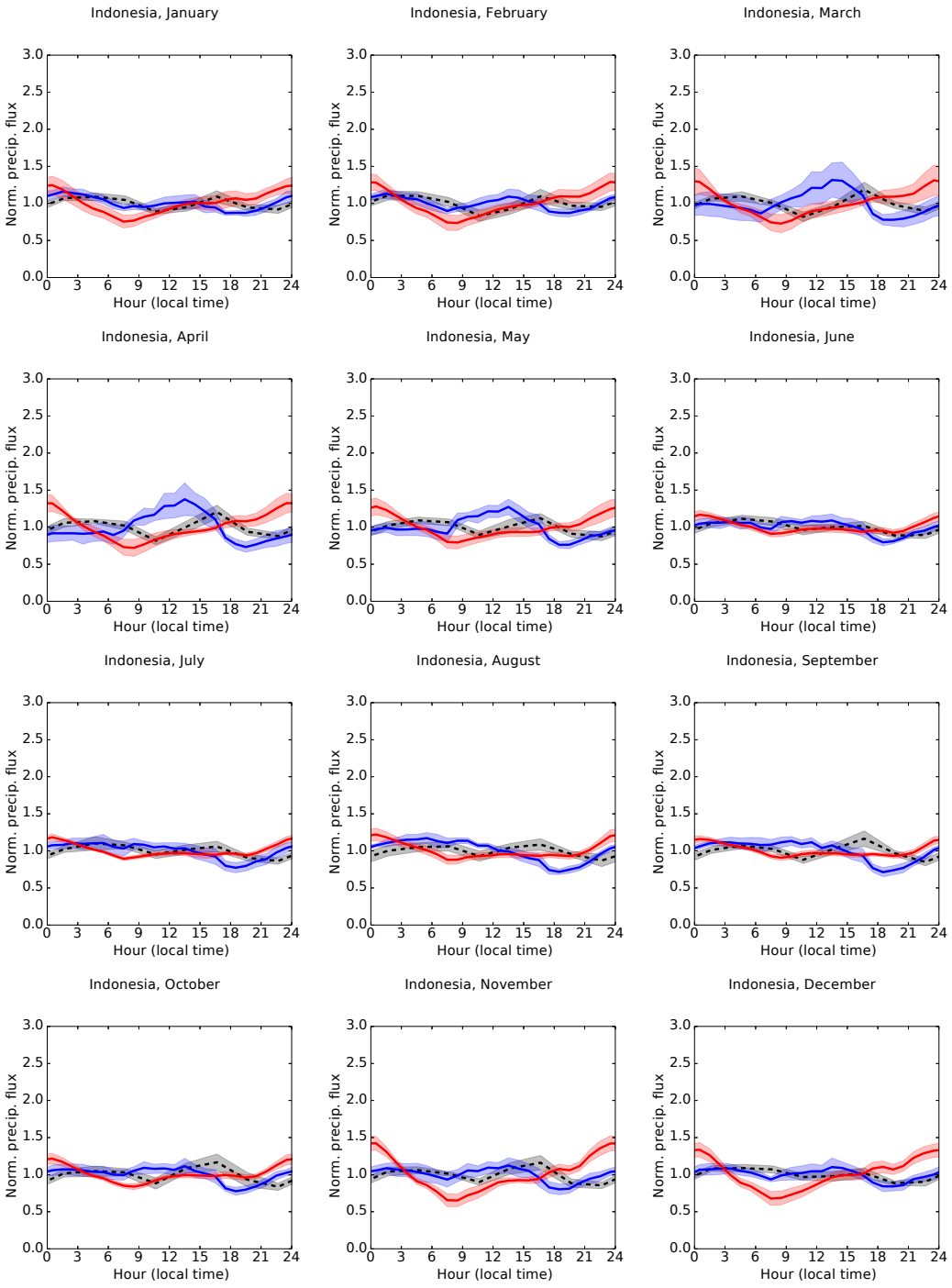

Figure S12: Normalised diurnal cycles of precipitation in the Indonesia region from a ten-year overlap between the TRMM 3B42 product and AMIP-type simulations using ECHAM (without HAM) with Tiedtke–Nordeng and CCFM (L−2) convection. The shaded regions indicate the interannual standard deviation of each data set. The dotted lines show the cycles from one-year simulations using alternative CCFM configurations. The diurnal cycles are in the local time of each region. Line colours and styles as per Figure S6.